The Journal *of* Immunology

Interaction with FcγRIIB Is Critical for the Agonistic Activity of Anti-CD40 Monoclonal Antibody

Ann L. White, H. T. Claude Chan, Ali Roghanian, Ruth R. French, C. Ian Mockridge, Alison L. Tutt, Sandra V. Dixon, Daniel Ajona, J. Sjef Verbeek, Aymen Al-Shamkhani, Mark S. Cragg, Stephen A. Beers and Martin J. Glennie

---

References
This article **cites 54 articles**, 27 of which you can access for free at:
http://www.jimmunol.org/content/187/4/1754.full#ref-list-1

Subscription
Information about subscribing to *The Journal of Immunology* is online at:
http://jimmunol.org/subscription

Permissions
Submit copyright permission requests at:
http://www.aai.org/About/Publications/JI/copyright.html

Email Alerts
Receive free email-alerts when new articles cite this article. Sign up at:
http://jimmunol.org/alerts

Interaction with FcγRIIB Is Critical for the Agonistic Activity of Anti-CD40 Monoclonal Antibody

Ann L. White,* H. T. Claude Chan,* Ali Roghanian,* Ruth R. French,* C. Ian Mockridge,* Alison L. Tutt,* Sandra V. Dixon,* Daniel Ajona,* J. Sjef Verbeek,[†] Aymen Al-Shamkhani,* Mark S. Cragg,* Stephen A. Beers,*,[1] and Martin J. Glennie*,[1]

A high activatory/inhibitory FcγR binding ratio is critical for the activity of mAb such as rituximab and alemtuzumab that attack cancer cells directly and eliminate them by recruiting immune effectors. Optimal FcγR binding profiles of other anti-cancer mAb, such as immunostimulatory mAb that stimulate or block immune receptors, are less clear. In this study, we analyzed the importance of isotype and FcγR interactions in controlling the agonistic activity of the anti-mouse CD40 mAb 3/23. Mouse IgG1 (m1) and IgG2a (m2a) variants of the parental 3/23 (rat IgG2a) were engineered and used to promote humoral and cellular responses against OVA. The mouse IgG1 3/23 was highly agonistic and outperformed the parental Ab when promoting Ab (10–100-fold) and T cell (OTI and OTII) responses (2- to >10-fold). In contrast, m2a was almost completely inactive. Studies in FcγR knockout mice demonstrated a critical role for the inhibitory FcγRIIB in 3/23 activity, whereas activatory FcγR (FcγRI, -III, and -IV) was dispensable. In vitro experiments established that the stimulatory effect of FcγRIIB was mediated through Ab cross-linking delivered in trans between neighboring cells and did not require intracellular signaling. Intriguingly, activatory FcγR provided effective cross-linking of 3/23 m2a in vitro, suggesting the critical role of FcγRIIB in vivo reflects its cellular distribution and bioavailability as much as its affinity for a particular Ab isotype. In conclusion, we demonstrate an essential cross-linking role for the inhibitory FcγRIIB in anti-CD40 immunostimulatory activity and suggest that isotype will be an important issue when optimizing reagents for clinical use.   *The Journal of Immunology*, 2011, 187: 1754–1763.

Anti-cancer mAb, such as rituximab and alemtuzumab, have become essential treatments for many cancers (1, 2). Although there is much debate about exactly how these reagents function, it is agreed that interaction of the mAb Fc with FcγR on immune effector cells is critical (3–6). Studies in pre-clinical models show that binding to activatory FcγR promotes cell killing by Ab-dependent cell-mediated cytotoxicity and phago-cytosis, whereas interaction with the inhibitory FcγRII (FcγRII or CD32 in mice, FcγRIIB or CD32B in humans; hereafter referred to as FcγRIIB) is reported by some (3, 5, 7), but not all (8), to be detrimental to activity. Thus, mAb, including mouse IgG2a and human IgG1, with high activatory/inhibitory receptor binding (A/I) ratios appear optimal (4, 7, 9). Genetic profiling studies also support a critical role for activatory FcγR in mAb function in humans, as individuals homozygous for allotypes of FcγRIIA (CD32A) or FcγRIIIA (CD16A) with enhanced IgG Fc binding show better clinical outcomes in response to therapy (10–13). Thus, a current

focus is mAb engineering to increase activatory FcγR binding and A/I ratios (14, 15).

Other mechanisms, such as direct cell killing and complement-mediated cytotoxicity, which doubtless play important roles with different mAb (16, 17), may also influence isotype requirement. This is exemplified by a recent study (18) that showed that the in vivo tumoricidal activity of the anti-death receptor 5 (DR5) mAb drozitumab was dependent upon FcγR interaction. However, in this case, interaction was required for Ab cross-linking to promote DR5-mediated apoptosis rather than for recruitment of effector functions, and the effect could be mediated by either activatory or inhibitory FcγR (18). Another class of mAb in de-velopment as anticancer agents is immunostimulatory mAb as exemplified by the anti–CTLA-4 mAb, ipilimumab, recently ap-proved by the U.S. Food and Drug Administration for metastatic melanoma (19). Immunostimulatory mAb bind either agonisti-cally or antagonistically to receptors on immune effector cells and provide therapy by stimulating immunity and potentially over-coming tumor-induced immune tolerance (20–22). The isotype requirements and the role of FcγR interaction for this type of mAb have not been investigated but may also differ from those of direct-targeting mAb, such as rituximab and alemtuzumab, that rely on effector cell recruitment.

Our work has focused on immunostimulatory anti-CD40 mAb (20, 23–25), which are also in clinical development (26, 27). Re-agents targeting this molecule have been investigated for >20 y and include both mAb and CD40L (20, 26). CD40 is a TNFR superfamily member expressed on APC, such as B cells, macro-phages, and dendritic cells (DC), as well as many nonimmune cells and a wide range of tumors (28–30). Interaction with its trimeric ligand on activated T cells results in APC activation, required for the induction of adaptive immunity (28, 29). In pre-clinical models, rat anti-mouse CD40 mAb show remarkable

*Division of Cancer Sciences, Faculty of Medicine, University of Southampton, Southampton SO16 6YD, United Kingdom; and †Department of Human Genetics, Leiden University Medical Center, Leiden 2333 ZA, The Netherlands

[1]S.A.B. and M.J.G. are the senior authors and contributed equally to this work.

Address correspondence and reprint requests to Prof. Martin J. Glennie and Dr. Ann L. White, Tenovus Research Laboratory, Southampton General Hospital, Tremona Road, Southampton, SO16 6YD, United Kingdom. E-mail addresses: mjg@soton.ac.uk and alw1@soton.ac.uk

Abbreviations used in this article: 7AAD, 7-aminoactinomycin D; A/I, activatory/inhibitory receptor binding; CHO, Chinese hamster ovary; DC, dendritic cells; DR5, death receptor 5; IKK, IκB kinase; m1, mouse IgG1; m2a, mouse IgG2a; MHC II, MHC class II; RU, resonance unit; WT, wild-type.

therapeutic activity in the treatment of CD40 positive B cell lymphomas as well as various CD40-negative tumors (20, 24, 25). In our studies of therapeutic mAb, their potency is unprecedented, clearing bulk tumors from mice with established disease and providing immunity to rechallenge (20, 24). To date, four anti-CD40 mAb [CP-870,893 (31), SGN-40 (32), HCD122 (26, 33)], and Chi LOB7-4 (34) have been investigated in phase I/II trials. These reagents show diverse activities ranging from antagonist (HCD122) to strong agonist (CP-870,893) (26). Currently, there is no satisfactory explanation for this heterogeneity, with little evidence for epitope specificity being the determining factor.

In this study, we investigated the effect of mAb isotype on the immunostimulatory activity of anti-CD40. Previous preclinical studies have focused on rat [3/23 and FGK45 (20, 22)] and hamster [IC10 (35)] anti-CD40 mAb. To address the role of isotype and to avoid possible interference from mouse anti-rat Ig responses, we engineered the epitope-binding (variable) regions of 3/23 onto mouse IgG1 (m1) or mouse IgG2a (m2a) constant regions. Importantly, both mAb retained equivalent binding to CD40 and were biologically active in vivo and in vitro. However, we discovered profound and unexpected differences in their immunostimulatory properties. When used to stimulate immunity to OVA, 3/23 m1 promoted a dramatic increase in both humoral and cell-mediated responses, whereas 3/23 m2a had almost no stimulatory effect. Strikingly, we found that interaction with the normally inhibitory FcγRIIB was required for 3/23 m1 stimulatory activity. These data not only indicate that isotype is critical for anti-CD40 mAb efficacy, but also that its requirements are entirely different from those of direct-targeting mAb such as rituximab.

Materials and Methods

Mice

C57BL/6, OTII TCR transgenic, and RAG$^{-/-}$ mice were sourced from Charles River Laboratories (Kent, U.K.). Other genetically altered strains used were FcγRIIB$^{-/-}$, FcRγ$^{-/-}$, CD40$^{-/-}$ (from Prof. Caetano Reis e Sousa, London, U.K.), C57BL/6-Tg(IghelMD4)4Ccg/J (MD4) (from Richard Cornall, Oxford, U.K.), and OTI TCR transgenic C57BL/6 mice (from Dr. Matthias Merkenschlager, Imperial College, London, U.K.). Animals were bred and housed in a local animal facility and were used at ~8–12 wk of age. All experiments were carried out according to local ethical committee guidelines under United Kingdom Home Office license number PPL30/2451.

Abs and reagents

The following hybridomas were used: rat anti-CD40 (clone 3/23; rat IgG2a) was originally a gift from Gerry Klaus (National Institute of Medical Research, London, U.K.); anti-rat CD4 (OX68) was a gift from Neil Barclay (Oxford University, Oxford, U.K.); and anti-mouse FcγRII/III (2.4G2), anti-mouse MHC class II (MHC II; M5/114.15.2), anti-mouse CD80 (1610A1), and anti-mouse CD86 (GL1) were from LGC (Teddington, U.K.). Anti-mouse FcγRI (AT152), FcγRIIB (AT130 and AT128), FcγRIII (AT154), and FcγRIV (CD16-2; AT137) were produced in-house (A.L. Tutt, S. James, S. Dixon, M. Ashton-Key, R. French, J. Teeling, E. Williams, A. Roghanian, C.I. Mockridge, S.A. Beers, M.S. Cragg, and M.J. Glennie, manuscript in preparation). Purified IgGs were prepared as described (16). All preparations were endotoxin low (<1 ng endotoxin/mg) as determined using the Endosafe-PTS portable test system (Charles River Laboratories).

Polyclonal rabbit anti-OVA was from Millipore (Watford, U.K.). Anti-CD19–PE (clone 1D3) and anti-F4/80–allophycocyanin were from AbD Serotec (Oxford, U.K.). Anti-mouse CD23-PE was from BD Biosciences. For OTII cell staining, anti-mouse Vα2–TcR:FITC (clone B20.1), anti-mouse Vβ5.1,5.2 TcR:PE (clone MR9-4, IgG1), and allophycocyanin-labeled anti-CD4 (clone RM4-5; all from BD Biosciences) were used. For OTI cell staining, allophycocyanin-labeled anti-CD8α (clone 53-6.7; BD Biosciences) and PE-labeled SIINFEKL tetramers were used. Tetramers were produced essentially as described (36) by the Cancer Research UK/Experimental Cancer Medicine Centre Protein Core Facility (Cancer Sciences Division, University of Southampton, Southampton, U.K.) with the following modifications: solubilized inclusion bodies were refolded in the presence of SIINFEKL peptide (Peptide Synthetics, Fareham, U.K.) at

~15 μM peptide, 4 μM mouse β$_2$-microglobulin, and 2 μM H-2K^b. PE-labeled streptavidin MHC class I tetramers were purified further on a Superdex TM 200 10/300GL gel filtration column in PBS, dialyzed against 16% glycerol in PBS, and stored in the presence of 0.5% BSA and 0.1% sodium azide at −20°C.

Chicken OVA was purchased from Sigma-Aldrich (Poole, U.K.). Endotoxin-free OVA was from Profos (Regensberg, Germany). 3/23 [Fab′ × OVA] derivatives, consisting of a single molecule of OVA chemically linked to one, two, or three Fab′ fragments, were prepared as previously described (37) and contained <0.5 ng endotoxin/mg conjugate.

Production of 3/23 chimeric mAb

DNA encoding the 3/23 H and L chain V regions was amplified from 3/23 hybridoma cDNA by PCR using Pfu DNA polymerase (Promega). The DNA fragments were sequenced and cloned into PCR-Blunt II TOPO vector (Invitrogen, Paisley, U.K.) containing the m1 or m2a constant regions via HindIII/SpeI sites (H chain) and HindIII/BSiWI sites (L chain). The two chains were then further subcloned into the expression vector pEE14.1 (Lonza). For mAb production, expression vectors were transfected into Chinese hamster ovary (CHO)-K1 cells using GenePorter (Genlantis, San Diego, CA) and cells secreting the highest amount of engineered Ab selected. Ab was purified from cell-culture media on a protein A-Sepharose (Sigma-Aldrich) column. All preparations were endotoxin low (see above).

Tissue culture

Cells were cultured at 37°C in a humidified atmosphere under 5% CO$_2$. Mouse primary B cells and splenocytes were cultured in RPMI 1640 containing 10% FCS, 2 mM glutamine, 1 mM sodium pyruvate, 100 U/ml penicillin, 100 μg/ml streptomycin (all from Life Technologies, Invitrogen), and 50 μM 2-ME (Sigma-Aldrich). CHO cells were cultured in GMEMS (First Link, Birmingham, U.K.) containing 5% dialyzed FCS, 2 μg/ml amphotericin B (Fungizone; Invitrogen), 100 U/ml penicillin, 100 μg/ml streptomycin, and 3 μM methionine sulfoximine (Sigma-Aldrich). Freestyle 293F cells (Life Technologies) were cultured according to the manufacturer's instructions. Mouse IIA1.6 B cell lymphoma cells transfected with various forms of mouse FcγRIIB, some lacking intracellular domains (A. Roghanian and M.S. Cragg, unpublished observations), were maintained in RPMI 1640 as above, plus 1 mg/ml G418 (Geneticin; Invitrogen).

Immunization and assessment of immune responses

Mice were immunized via tail vein injection in 200 μl saline as described for individual experiments. Anti-OVA Ab levels in serum samples were determined by ELISA as previously described (38). To analyze T cell responses, mice were adoptively transferred with ~1 × 10^6 OVA-specific CD8 (OTI) or CD4 (OTII) splenic T cells via tail vein injection the day before immunization. Numbers of circulating OVA-specific T cells in blood or in the spleen were determined by flow cytometry using an FACSCalibur (BD Biosciences).

Phagocytosis assay

Bone marrow-derived macrophages (6) were plated into flat-bottomed 96-well dishes (5 × 10^4 per well) and left to adhere at 37°C for 2 h. Mouse splenic B cells were purified by negative selection (Miltenyi Biotec, Surrey, U.K.) and labeled for 15 min at room temperature with 5 μM CFSE. B cells were then coated with 3/23 m1 or m2a or isotype control mAb at 10 μg/ml for 20 min at room temperature, washed, and added to the macrophages at a ratio of 5:1 B cells/macrophages. After 1 h at 37°C, macrophages were labeled with anti-F4/80–allophycocyanin (macrophage marker) and the number of double-positive (CFSE$^+$F4/80$^+$) cells identified by flow cytometry.

Immunohistochemistry

CD70 staining was performed as previously described (39). Briefly, 10-μm frozen spleen sections were fixed in acetone, blocked with 5% normal goat serum, and incubated with biotinylated rat anti-CD70 (BD Biosciences) overnight at 4°C. Tyramide signal amplification was used to enhance the CD70 staining (TSA Kit No. 22; Invitrogen) followed by streptavidin-conjugated Alexa Fluor 488 (Molecular Probes). Sections were mounted in Vectashield containing DAPI (Vector Laboratories, Burlingame, CA). Images were collected on a Leica TCS SP2 confocal laser scanning microscope (Leica Microsystems) using argon (488 nm), green helium/neon (543 nm), and red helium/neon (633 nm) lasers and a pinhole equivalent to 1 Airy disc. Image files (.tiff) were transferred to Adobe Photoshop CS2 (Adobe Systems).

B cell proliferation, activation, and survival

To analyze proliferation, total splenocytes or splenic B cells purified by negative selection (Miltenyi Biotec) were plated into 96-well round-bottom dishes at 1×10^5 cells/well in a total volume of 200 μl containing various concentrations of mAb as described for individual experiments. In some cases, 1×10^5 transfected cells (see below) were also added. Cells were incubated at 37°C for 5 d. During the final 16 h, (methyl-[^{3}H]thymidine; PerkinElmer, Cambridge, U.K.) was added (0.5 μCi/well). Cells were harvested using a Packard Filtermate Harvester 96 (PerkinElmer) and counted.

To analyze activation status, splenic B cells were purified and plated into 96-well dishes as described above. After 48 h at 37°C, cells were harvested and the expression of activation markers analyzed by flow cytometry. Surviving B cells were assessed through exclusion of 7-aminoactinomycin D (7AAD; BD Biosciences) staining.

For NF-κB signaling analysis, isolated wild-type (WT) C57BL/6 B cells were plated in 12-well plates (~2×10^6/ml/well) and stimulated with 10 μg/ml 3/23 m1 or m2a for 2, 5, 15, and 30 min at 37°C. For caspase-8 analysis, isolated WT and FcγRIIB$^{-/-}$ splenic BALB/c B cells were stimulated with 10 μg/ml mAb overnight at 37°C. Cell lysates were prepared for Western blotting as described (40) and 25–35 μg samples resolved by denaturing SDS-PAGE, transferred onto polyvinylidine difluoride membranes, and then incubated with Abs to phospho-IκB kinase (IKK) α/β (Ser$^{176/180}$; clone 16A6), phospho–IκB-α (Ser32/36; clone 5A5), anti-tubulin, β-actin (all from Cell Signaling Technologies), IκB-α (Santa Cruz Biotechnology, Santa Cruz, CA), and caspase-8 (kindly provided by Dr. Lorraine O'Reilly, Walter and Eliza Hall Institute, Melbourne, Australia) followed by HRP-conjugated secondary Ab. Blots were visualized using ECL reagents (GE Healthcare, Buckinghamshire, U.K.).

Transfections

DNA fragments encoding mouse FcγRs were amplified from mouse splenocytes and peripheral blood cDNA. After verifying their sequences, they were subcloned into the expression vector pCIpuro via EcoRI and NotI sites. The backbone vector pCI-puro was made by replacing the neomycin resistance cassette from pCI-neo (Clontech, Basingstoke, U.K.) with the puromycin resistance gene from pPUR (Clontech). Mouse γ-chain was subcloned into the expression vector pcDNA3 (Invitrogen) via HindIII and EcoRI sites. Plasmids were transfected into 293F cells using the 293fectin transfection reagent (Invitrogen). A total of 10 μg DNA was used with 1×10^7 cells. For the activatory receptors (I, III, and IV), 5 μg appropriate α-chain and 5 μg γ-chain DNA was used. FcγR expression was assessed by flow cytometry 72 h later.

Surface plasmon resonance

A Biacore T100 (Biacore) was used to assay the interaction between soluble FcγR and 3/23 m1 or m2a. Abs or BSA as a control were immobilized at high (15,000 resonance units [RU]) and low (1,000 RU) densities to the flow cells of CM5 sensor chips (Biacore) by standard amine coupling according to the manufacturer's instructions. Soluble Fc receptors (FcγRI, -IIB, -III, and -IV; R&D Systems, Abingdon, U.K.) were injected through the flow cell at 200, 100, 50, 25, 12.5, and 6.25 nM (50 nM point in duplicate) in HBS-EP running buffer (Biacore) at a flow rate of 30 μl/min. Soluble Fc receptors were injected for 5 min, and dissociation was monitored for 10 min. Background binding to the control flow cell was monitored automatically. Affinity constants were derived from the data by equilibrium binding analysis (FcγRIV and FcγRI to m2a) and/or analysis of association and dissociation using a 1:1 binding model as indicated using Biacore Bioevaluation software (Biacore).

Statistical analyses

Student t tests (unpaired) were performed using GraphPad Prism software (GraphPad Software, La Jolla, CA). For comparison of Ab responses, data were log-transformed before analysis. Significance was accepted when $p <$ 0.05.

Results

Characterization of m1 and m2a anti-mouse CD40 mAb

To examine the importance of mAb isotype in the immunostimulatory activity of anti-CD40, we cloned the variable regions of the rat anti-mouse CD40 mAb 3/23 (3/23 r2a) onto m1 and m2a constant regions and expressed the chimeric mAb in CHO cells. The purified mAb showed equivalent Ag-binding function, with

similar binding curves to cell-expressed mouse CD40 and competition with the parent 3/23 r2a for binding to B cells (Fig. 1A). The function of the Fc portion of each mAb was assessed through comparison of their binding to each of the mouse FcγR (I, IIB, III, and IV) using surface plasmon resonance (Fig. 1B). Consistent with reports in the literature (41), 3/23 m2a showed high-affinity binding to FcγRI and FcγRIV and bound much less well to FcγRIIB and -III (Fig. 1B). In contrast, 3/23 m1 showed no detectable binding to FcγRI and -IV and bound to FcγRIIB and -III (Fig. 1B) with relatively low affinity. Fig. 1C gives estimated K_D values for each interaction, which are similar to those previously reported (41). We also examined the ability of the mAb to enhance phagocytosis of opsonized B cells by macrophages in vitro (Fig. 1D). As expected from their FcγR binding profiles (42), 3/23 m2a promoted phagocytosis, whereas m1 did not (Fig. 1D). Importantly, both mAb were functional in vivo, with a 100-μg dose of either isotype causing a transient reduction in circulating B cells in mice and, in the case of 3/23 m1, causing an ~2-fold increase in spleen weight by day 7 after treatment (Fig. 1E), which is similar to that reported for 3/23 r2a (Fig. 1E) (20).

3/23 m1 but not m2a is an immunostimulator

To assess the influence of isotype on immunostimulatory function, we examined the ability of the 3/23 m1 and m2a mAb to stimulate adaptive immune responses (Fig. 2). A 100-μg dose of each mAb, or the parent r2a, was injected i.v. into mice along with the model Ag, OVA. For Ab responses, the OVA was administered either as immune complexes, free soluble protein (Sigma-Aldrich; contaminated with ~50 IU/mg endotoxin), or endotoxin-free soluble protein. For all forms of the Ag, 3/23 m1 caused a dramatic (from 10- to >100-fold) increase in circulating anti-OVA Ab levels by day 14. For immune complexes, this enhancement was greater than that observed for the parent r2a (Fig. 2A). In contrast, 3/23 m2a had no effect on the Ab response (Fig. 2A). Further experiments demonstrated that as little as 25 μg 3/23 m1 provided maximal stimulation of the Ab response, whereas as much as 500 μg m2a had no stimulatory effect (data not shown). In similar studies, 3/23 m1 but not m2a also increased anti–4-hydroxy-3-nitrophenyl Ab responses against OVA–4-hydroxy-3-nitrophenyl (data not shown).

To assess T cell responses, mice were adoptively transferred with OVA-specific CD4 (OTII) or CD8 (OTI) T cells then immunized as above with endotoxin-free OVA plus 3/23 mAb. Circulating numbers of OTII and OTI cells were followed over time. In addition, T cell numbers in the spleen were determined 4 d after immunization (Fig. 2B, 2C). For both CD4 and CD8 T cells, a small, transient increase in circulating numbers was observed in control mice that was not influenced by the presence of 3/23 m2a. In contrast, 3/23 m1 promoted a 2- and 11-fold increase in circulating CD4 and CD8 T cells, respectively. Similarly, 3/23 m2a had no effect on numbers of OVA-specific CD8 T cells in the spleen, although it caused a small, but significant, increase in splenic CD4 T cell numbers. In contrast, 3/23 m1 caused a dramatic 5- and 21-fold increase in OVA-specific splenic CD4 and CD8 T cells, respectively (Fig. 2B, 2C, insets). Thus, for both arms of the adaptive immune response, 3/23 m1, but not 3/23 m2a, was able to provide stimulation.

Differential effects of anti-CD40 mAb on activation of DC and B cells

Ligation of CD40 on APC plays an essential role in the initiation of adaptive immune responses (28, 29). Two key APC that express CD40 are DC and B cells. We therefore examined the effect of the mAb on these APC in vivo and in vitro. Consistent with their
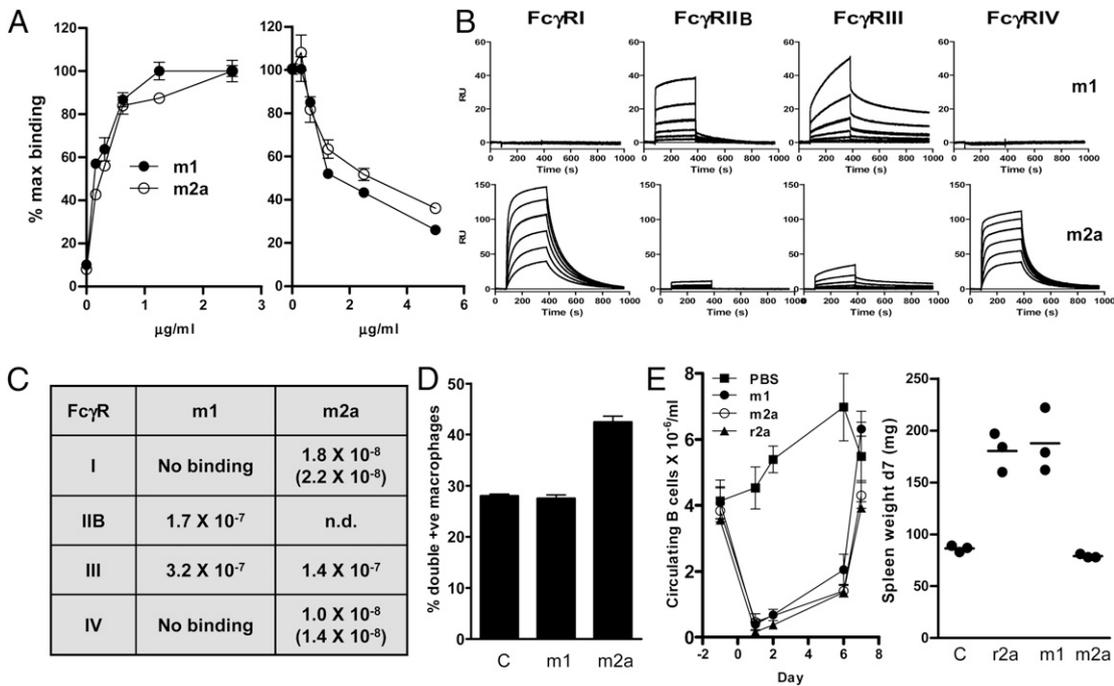
FIGURE 1. Characterization of m1 and m2a forms of 3/23 anti-mouse CD40. *A*, Mouse B cells [π-BCL$_1$ (54)] were incubated with increasing concentrations of 3/23 m1 or m2a followed by goat anti-mouse IgG Fc-FITC (*left panel*) or in the presence of 1 μg/ml 3/23 rat IgG2a-FITC (*right panel*). Cells were analyzed by flow cytometry for FITC labeling. Results are presented as mean fluorescence intensity ± SE of triplicate samples and represent one of at least two experiments. *B*, Surface plasmon resonance analysis of 3/23 m1 and m2a binding to mouse FcγR. Recombinant, soluble FcγR proteins (0, 6.25, 12.5, 25, 50, 50, 100, and 200 nM) were passed over 3/23 mAb immobilized at 1000 RU. Sensograms are shown. Similar results were obtained with mAb immobilized at 15,000 RU. *C*, Calculated K_D values for interactions shown in *B*. *D*, Phagocytosis of fluorescently labeled mouse B cells, uncoated (C) or coated with 3/23 m1 or m2a, by bone marrow-derived macrophages. Results are mean ± SEM for quadruplicate samples and represent one out of two experiments. *E*, Mice were injected with a 100-μg dose of 3/23 mIgG1 or mIgG2a in PBS or with PBS alone (C). *Left panel*, Numbers of circulating B cells were followed over time (mean ± SD of three mice). *Right panel*, Spleen weights were determined on day 7. Results are representative of one out of three experiments. n.d., not determined, as binding level too low.

differential effects on immune responses (Fig. 2), 3/23 r2a and m1 increased the expression of CD70 on splenic DC (Fig. 3*A*) and promoted proliferation of B cells (Fig. 3*B*) in vivo. In contrast, although a small increase in CD70 expression on DC was observed in response to 3/23 m2a (Fig. 3*A*), this mAb had no effect on B cell proliferation in vivo (Fig. 3*B*). In addition, 3/23 r2a and m1, but not m2a, promoted robust proliferation of isolated B cells in vitro (Fig. 3*C*), an assay commonly used to assess the agonistic activity of anti-CD40 mAb. 3/23 m1 also promoted greater up-regulation of activation markers on B cells as assessed by expression of CD23, CD80, CD86, and MHC II (Fig. 3*D*) and a higher phosphorylation of IKKα/β and IκB-α proteins than m2a (Fig. 3*E*), leading to reduced levels of IκB in a time-dependent manner, which is suggestive of higher NF-κB activation in these cells (43). Interestingly, both forms of the Ab were equally able to promote B cell survival in vitro (Fig. 3*F*), consistent with studies showing differential requirements for anti-CD40–induced B cell proliferation and rescue from apoptosis (44). Thus, as measured by several different approaches, 3/23 m1 and r2a promoted much greater activation of APC in vitro and in vivo than m2a, which may explain their differential effects on immune responses.

Essential role for FcγRIIB in the immunostimulatory activity of anti-CD40

FcγR mediate many Ab functions in vivo, and activatory FcγR, particularly FcγRIIA and -IIIA in humans [FcγRIII and IV in mice (45)], are crucial in providing the efficacy for rituximab and other anti-cancer mAb. To determine the role of FcγR in the agonistic activity of 3/23 and whether isotype differences in FcγR interaction were responsible for the contrasting effects of 3/23 m1

and m2a on immune responses, we analyzed anti-OVA Ab responses in FcγR$^{-/-}$ mice. Two strains were used; FcγRIIB$^{-/-}$ mice, which lack the inhibitory receptor but have all of the activatory FcγR (I, III, and IV) intact (46); and FcR$\gamma^{-/-}$ mice, which lack all activatory FcγR but retain the inhibitory FcγRIIB (47). Despite some variation in response among animals, 3/23 m1 caused a very large and significant increase in Ab titers in both WT and FcR$\gamma^{-/-}$ mice, whereas this effect was lost in FcγRIIB$^{-/-}$ mice (Fig. 4*A*).

Consistent with the in vivo data, 3/23 m1 stimulated robust proliferation of B cells in splenocyte cultures in vitro (Fig. 4*B*). Loss of activatory receptors in FcR$\gamma^{-/-}$ splenocyte cultures did not impact the ability of 3/23 m1 to stimulate B cell proliferation in vitro, whereas loss of FcγRIIB abrogated its effect (Fig. 4*B*). In contrast, 3/23 m2a allowed only a low level of proliferation in WT, FcR$\gamma^{-/-}$, and FcγRIIB$^{-/-}$ cultures (Fig. 4*B*).

Results in Fig. 4*A* and 4*B* suggest that FcγRIIB plays an essential role in delivering the agonistic activity of 3/23 and that activatory FcγR are not required. Thus, isotype differences in anti-CD40 activity may be explained by differences in the affinity of 3/23 m1 and m2a for FcγRIIB (Fig. 1*B*, 1*C*) (41).

To examine the role of FcγRIIB further, we determined the effects of the 3/23 mAb on purified B cells in vitro where FcγRIIB is the only FcγR expressed. Consistent with the data in Fig. 4*B*, 3/23 m1 stimulated robust proliferation of WT B cells but not FcγRIIB$^{-/-}$ B cells, whereas 3/23 m2a did not stimulate proliferation of either (Fig. 4*C*). LPS stimulation resulted in proliferation of both WT and FcγRIIB$^{-/-}$ B cells and to a similar extent (Fig. 4*C*, *inset*), demonstrating that the FcγRIIB$^{-/-}$ B cells were capable of dividing. Furthermore, two different anti-mouse
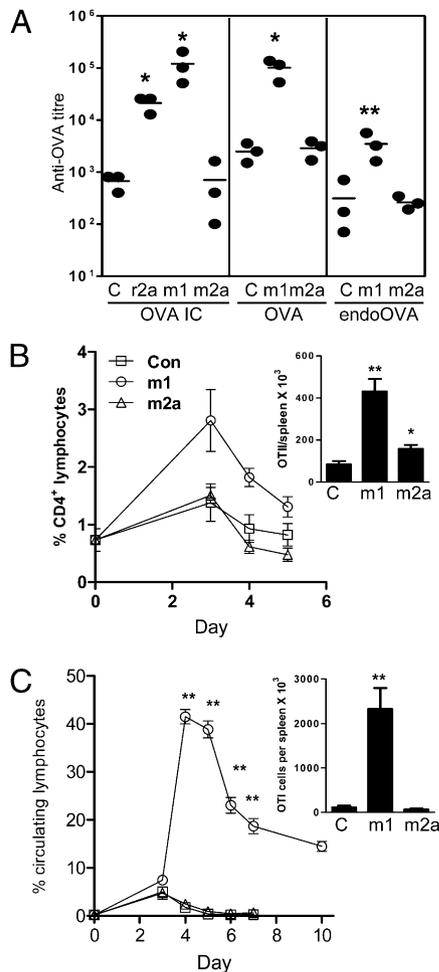
FIGURE 2. 3/23 m1 but not m2a is immunostimulatory. *A*, C57BL/6 mice were injected with 100 μg OVA immune complexes (IC), 0.5 mg soluble OVA (Sigma-Aldrich), or 50 μg endotoxin-free (endo) OVA, plus 100 μg isotype control m1 (C), 3/23 m1, m2a, or r2a, as indicated. Circulating levels of anti-OVA Ab were determined 7 (OVA IC) or 14 d later. Results for individual mice are shown and represent one out of three experiments for each Ag. Mice were adoptively transferred with OVA-specific CD4 (OTII) (*B*) or CD8 (OTI) (*C*) T cells on day 1, then immunized with 50 μg endoOVA plus 100 μg control m1, 3/23 m1, or m2a on day 0. Circulating numbers of OTII and OTI cells were determined over time in serial bleeds. Results are mean ± SD for three animals and represent one out of three (*B*) or four (*C*) experiments. *Insets* show numbers of OTII/OTI T cells in the spleens day 4 after immunization and are mean ± SD for three animals. *$p < 0.05$, **$p < 0.001$ versus control.

FcγRIIB mAb blocked the ability of 3/23 m1 to stimulate proliferation of WT B cells (Fig. 4*D*). Consistent with the isotype-independent role of 3/23 in promoting B cell survival (Fig. 3*F*), the loss of FcγRIIB did not prevent 3/23 m1 from increasing cell survival (Fig. 4*E*). In contrast, activation of B cells, as measured by increased expression of MHC II (Fig. 4*F*) or caspase-8 activation (Fig. 4*G*), was reduced.

The role of FcγRIIB is in Ab cross-linking

Using B cell proliferation as a readout of activity, we took a number of approaches to determine the role that FcγRIIB plays in 3/23 activity. First, we compared the ability of immobilized 3/23 m1 and m2a to promote the proliferation of WT and FcγRIIB$^{-/-}$ B cells. Under these conditions, both mAb provided equivalent and effective stimulation, with levels of proliferation similar in WT and FcγRIIB$^{-/-}$ cultures (Fig. 5*A*). Thus, when immobilized

to simulate cross-linking, the dependence on FcγRIIB interaction was lost, and both mAb became effective agonists.

Second, we determined the ability of a truncated FcγRIIB that lacked its intracellular tail to enhance anti-CD40 activity. The intracellular domain of FcγRIIB contains an ITIM signaling motif that mediates its regulatory effects on immune responses (48). Control-transfected FcγR-negative mouse IIA1.6 B cell lymphoma cells and IIA1.6 cells transfected with either full-length mouse FcγRIIB (b1 isoform) or its tailless equivalent (FcγRIIB-SLV) were treated with 3/23 m1 or m2a and their activation status examined. 3/23 m1 was more potent than 3/23 m2a at inducing activation of both forms of FcγRIIB-transfected IIA1.6 cell lines, as suggested by higher upregulation of MHC II (not shown) and CD23 cell-surface expression (Fig. 5*B*). Thus, intracellular signaling through FcγRIIB was not required for this activity.

Third, we examined the ability of 3/23 [Fab′ × OVA] conjugates (37, 38) to stimulate B cell proliferation. [Fab′ × OVA] conjugates consisted of a single molecule of OVA chemically cross-linked to one, two, or three 3/23 Fab′ fragments (3/23 [F(ab′)$_1$ × OVA], [F(ab′)$_2$ × OVA], and [F(ab′)$_3$ × OVA], respectively). Addition of [3/23 F(ab′)$_3$ × OVA] stimulated proliferation of WT B cells to a similar extent as 3/23 m1 (Fig. 5*C*), whereas [3/23 F(ab′)$_1$ × OVA] and [3/23 F(ab′)$_2$ × OVA] were much less effective and showed similar activity to 3/23 m2a. This is interesting, as CD40-driven responses are initiated following binding to a trimeric CD40L (CD154) (49). [3/23 F(ab′)$_3$ × OVA] was also effective in stimulating the proliferation and activation of both FcγRIIB$^{-/-}$ B cells and MyD88$^{-/-}$/Toll/IL-1R domain-containing adapter inducing IFN-β$^{-/-}$ B cells (data not shown).

Finally, we determined whether FcγRIIB needed to be expressed on the same cell as CD40 to provide cross-linking. For this, we prepared purified CD40$^{-/-}$ and FcγRIIB$^{-/-}$ B cells and analyzed their ability to proliferate in response to 3/23 m1 when cultured alone or mixed together. As expected, neither cell type proliferated when cultured alone. However, when mixed together, robust proliferation was observed (Fig. 5*D*). As expected, proliferation was attributable to the FcγRIIB$^{-/-}$ (CD40$^{+/+}$) cells, as prior irradiation of the FcγRIIB$^{-/-}$ cells prevented radiolabel incorporation in mixed cultures, whereas irradiation of the CD40$^{-/-}$ cells did not (Fig. 5*D*). Interestingly, the level of proliferation observed in the mixed cultures was similar to that seen for WT B cells, suggesting that FcγRIIB is maximally effective when present on neighboring cells (Fig. 5*D*).

In summary, the results presented in Fig. 5 demonstrate that the role of FcγRIIB in anti-CD40 activity is one of cross-linking, that intracellular signaling through FcγRIIB is not required, and that its presence on a neighboring cell is sufficient to provide activity.

Other FcγR can also provide cross-linking for anti-CD40

The cross-linking role of FcγRIIB raises the question as to why other FcγR do not provide effective cross-linking for 3/23 m2a in vivo, as this binds to FcγRI and -IV with much higher affinity than 3/23 m1 does to FcγRIIB (Fig. 1*B*, 1*C*). Thus, the dominant role of FcγRIIB in anti-CD40 activity in vivo must either reflect specific properties of this receptor that make it particularly adept at cross-linking anti-CD40 mAb or its specific pattern and/or level of expression. To address this issue, we assessed the ability of all four mouse FcγR to provide effective cross-linking for 3/23 m1 and m2a when expressed in vitro. 293F cells transfected with each receptor (Fig. 6*A*) were cocultured with 3/23 mAb and FcγRIIB$^{-/-}$ B cells and the level of B cell proliferation assessed (Fig. 6*B*). Consistent with the surface plasmon resonance data (Fig. 1*B*, 1*C*), FcγRIIB and -III stimulated proliferation of B cells in the presence of 3/23 m1 to a similar extent, whereas FcγRI and IV
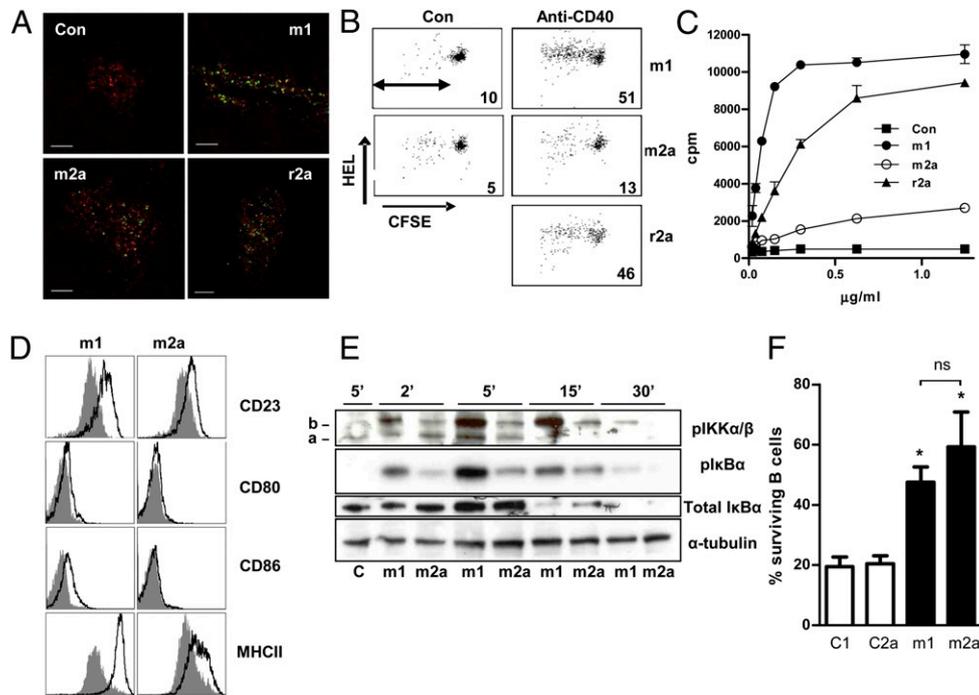
FIGURE 3. Differential effects of anti-CD40 mAb on activation of APC. *A*, C57BL/6 RAG$^{-/-}$ mice were injected with 100 μg isotype control m1 (Con) or 3/23 m1, m2a, or r2a as indicated. Two days later, spleens were removed and sections stained for CD70 (green) and the DC marker miDC8 (red). RAG$^{-/-}$ mice were used as CD70 expression is more easily visualized in these mice; however, similar results were obtained in WT animals (not shown). Scale bars, 50 μm. *B*, Mice injected with CFSE-labeled hen egg lysozyme (HEL)-specific purified splenic B cells received 100 μg indicated mAb. Four days later, spleens were removed and CFSE-labeled B cells analyzed by flow cytometry after intracellular staining with HEL-FITC to visualize the transferred cells. Plots are gated on CD19$^+$ lymphocytes and are representative of one out of four experiments performed in duplicate. *Inset* arrow in Con panel indicates region containing divided cells. Similar results were obtained with WT B cells (not shown). *C*, Purified splenic B cells were incubated with increasing concentrations of the indicated mAb for 5 d. Incorporation of [^{3}H]thymidine was assessed during the final 16 h. Results are mean ± SEM of triplicate samples and show results from 1 out of >10 experiments. *D*, Expression of activation markers on purified splenic B cells incubated with 1 μg/ml m1 or m2a isotype control mAb (filled histogram) or 3/23 m1 or m2a (black line) for 48 h. Results from one out of five experiments are shown. *E*, Western blot of lysates from B cells treated for the indicated times with 3/23 m1 or m2a probed with Ab specific for phospho-IKKα/β, phospho-IκB-α, or IκB-α. Anti-tubulin was used as a loading control. *F*, B cells incubated as in *D* were analyzed by staining with 7AAD and flow cytometry to determine the percentage of live (7AAD-negative) cells. Results are mean ± SE of quadruplicate samples and are representative of four experiments. *$p < 0.01$ versus control.

provided no stimulation (Fig. 6*B*). In contrast, all four FcγR were able to cross-link 3/23 m2a to stimulate proliferation (Fig. 6*B*). Surprisingly, the order of effectiveness did not correlate with the relative FcγR binding affinity, as although FcγRI was the most effective, FcγRIV was the least despite similar high-affinity binding (Fig. 6*B*). In addition, FcγRIIB was able to provide effective cross-linking for 3/23 m2a in these experiments (Fig. 6*B*). In contrast, cell lines expressing lower levels of FcγRIIB (data not shown) or WT B cells that express FcγRIIB (Fig. 2*C*; level of FcγRIIB expression shown in the *inset* in Fig. 6*A*) were unable to cross-link m2a, suggesting that the level of FcγR expression is also important.

These experiments thus suggest that it is the bioavailability of FcγRIIB in vivo, rather than specific properties of this receptor, that dictates its dominant role in anti-CD40 activity.

Discussion

In this study, we have shown that interaction with the normally inhibitory FcγR, FcγRIIB, is a prerequisite for the in vivo immunostimulatory activity of anti-CD40 mAb. This is in stark contrast to the requirement of direct-targeting anti-cancer mAb, such as rituximab and alemtuzumab, in which activatory FcγR are required for efficacy and interaction with FcγRIIB may be detrimental to activity (2). This differential FcγR dependence is reflected in the optimally active isotype of each type of mAb in mouse models; thus, IgG2a is optimal for direct-targeting mAb, whereas in this study, we show that IgG1 is optimal for anti-CD40.

Current emphasis in the design of therapeutic mAb is focused upon the engineering of variants with high affinity for activatory FcγR (14, 15). Our data indicate this approach may not be appropriate for immunostimulatory mAb and thus has significant implications for the design of immunotherapeutic agents.

The essential role of FcγRIIB in the immunostimulatory activity of anti-CD40 is surprising, as this receptor normally plays an inhibitory role in the immune system (48). Detailed in vitro studies, however, showed that intracellular signaling through FcγRIIB was not required for mediating the effects of anti-CD40; rather the role of the receptor was in mAb cross-linking. As other FcγR bind mAb Fc with higher affinity than FcγRIIB (this study and Refs. 41, 50), we investigated whether they could also provide effective cross-linking in vitro. Indeed, the ability of the different mouse FcγR to effectively cross-link 3/23 m1 and m2a correlated with their Fc binding profiles. Thus, FcγRI, -II, -III, and -IV all provided cross-linking for 3/23 m2a, whereas only FcγRIIB and -III were effective for 3/23 m1. Interestingly, however, their relative effectiveness did not correlate with measured Fc affinities. For example, FcγRIIB and -III bound 3/23 m2a with >10-fold lower affinity than FcγRIV and yet provided more effective cross-linking in vitro, suggesting perhaps that some FcγR are more adept at cross-linking anti-CD40 than others. This could reflect properties of the receptors themselves or of the 3/23 mAb. Whether this is also true for other immunostimulatory mAb (e.g., anti-CD27, anti–4-1BB, and anti–CTLA-4) is a question we are actively investigating.
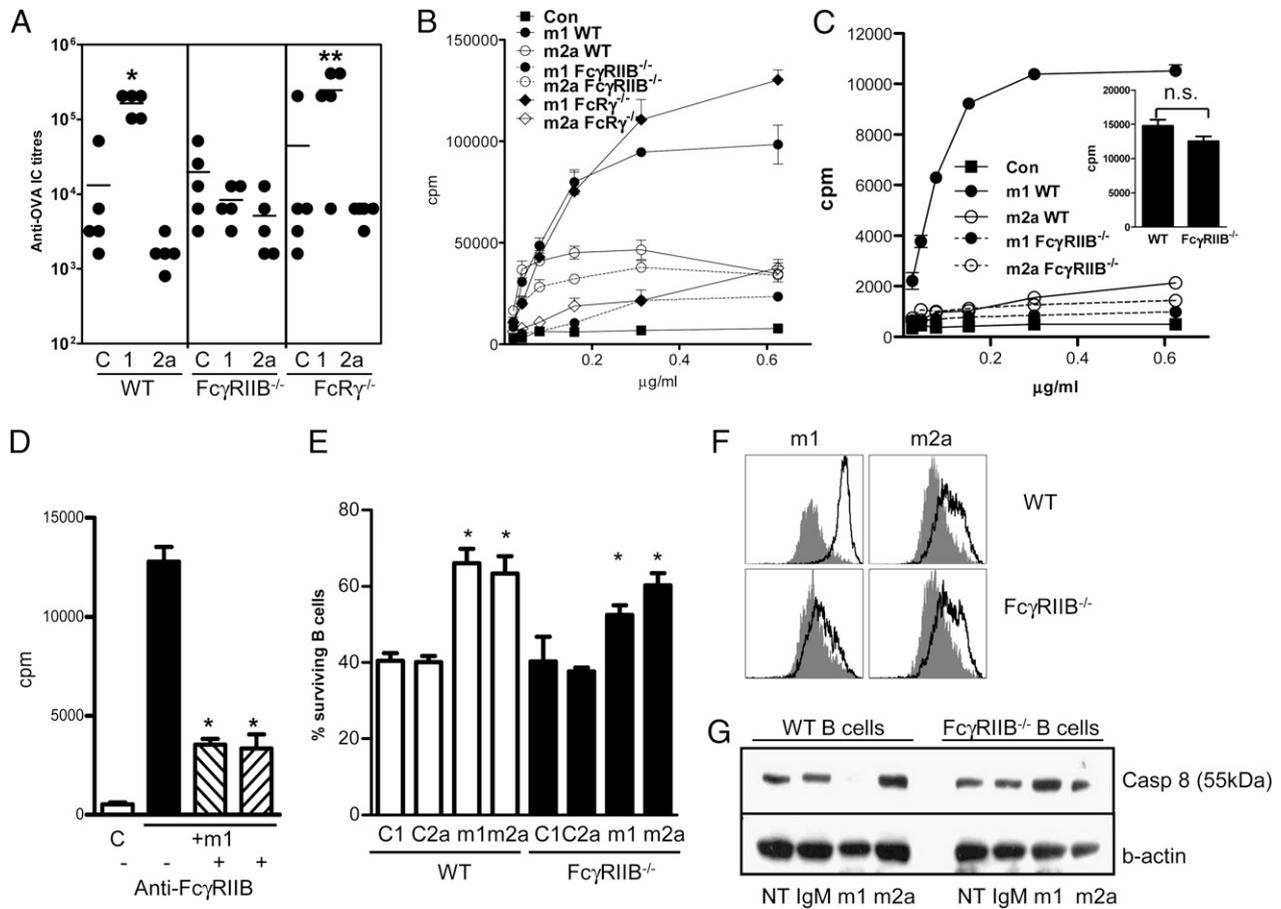
FIGURE 4. Essential role for FcγRIIB in the immunostimulatory activity of anti-CD40. *A*, WT, FcγRIIB$^{-/-}$, and FcRγ$^{-/-}$ C57BL/6 mice were immunized with 100 μg OVA IC plus 100 μg isotype control m1 (C) or 3/23 m1 or m2a. Day 7 anti-OVA Ab titers are shown for individual animals. *$p <$ 0.001, **$p <$ 0.05 versus control. *B*, B cell proliferation in splenocyte cultures from WT, FcγRIIB$^{-/-}$, and FcRγ$^{-/-}$ mice in response to 3/23 m1 or m2a analyzed as in Fig. 2C. Isotype m1 control is shown for WT splenocytes only. Results are mean ± SEM for triplicate samples and representative of two experiments. *C*, Proliferation of purified splenic B cells from WT or FcγRIIB$^{-/-}$ mice. Results are mean ± SEM of triplicate samples from one out of five experiments. *Inset* shows proliferation in response to 10 μg/ml LPS. *D*, Proliferation of WT B cells in response to 1 μg/ml control m1 (C) or 3/23 m1 in the absence or presence of 10 μg/ml two different anti-FcγRIIB mAbs, AT128 and AT130-5. Results are mean ± SEM of triplicate samples from one of two experiments. *$p <$ 0.001 versus 3/23 m1 alone. *E*, Percent of surviving WT and FcγRIIB$^{-/-}$ B cells after 48-h culture in the presence of isotype control (C) or 3/23 m1 or m2a mAb at 1 μg/ml. Data are mean ± SD of six samples from two different experiments. *$p <$ 0.01 versus isotype control. *F*, MHC II expression on WT and FcγRIIB$^{-/-}$ B cells incubated for 48 h with isotype control (filled gray histograms) or 3/23 m1 or m2a (black lines). Results are from one out of two experiments. *G*, WT and FcγRIIB$^{-/-}$ purified spenic B cells were not treated (NT) or incubated overnight with 10 μg/ml anti-mIgM, 3/23 m1, or m2a. The following day, cell lysates were analyzed by Western blotting for caspase-8 or β-actin as loading control.

In vitro studies also revealed that high levels of FcγRIIB expressed on transfected human fibroblasts were able to cross-link 3/23 m2a in vitro. Lower levels of FcγRIIB found on WT B cells (this study) or stable cell lines expressing the receptor (not shown), however, did not. Although we could detect minimal binding of 3/23 m2a to FcγRIIB, this was too low to calculate an accurate K_D value, consistent with the reported lower affinity of m2a versus m1 for FcγRIIB (41). The difference in activity between 3/23 m1 and m2a in vivo may thus reflect a threshold of affinity for FcγRIIB required for functional activity. These data suggest that expression levels and biodistribution of FcγRIIB, as well as Fc binding affinity, are important for its cross-linking function.

Interestingly, we have found that the parent 3/23 r2a mAb has a similar mouse FcγR binding profile to 3/23 m1 and that its ability to stimulate B cell proliferation in vitro is also dependent upon the presence of FcγRIIB (A.L. White, unpublished observations). More detailed analyses will be required to determine whether its reduced ability compared with 3/23 m1 to stimulate immunity is due to a lower affinity for FcγRIIB.

Wilson et al. (18) recently reported that FcγR interaction was required for the therapeutic activity of drozitumab (anti-DR5 mAb) in mice. As we have shown in this study for anti-CD40, the role of FcγR in this case was also in mAb cross-linking rather than effector cell recruitment (18). However, in contrast to the current study, either activatory or inhibitory FcγR could provide cross-linking for drozitumab in vivo. Interestingly, these authors also demonstrated that the ability of the rat anti-mouse CD40 mAb FGK-45 to stimulate NF-κB activation in isolated mouse B cells was lost in cells from FcγRIIB$^{-/-}$ mice (18). From these combined data, we hypothesize that for mAb that require FcγR-mediated cross-linking the location of target expression may determine the profile of FcγR dependence. DR5 is ubiquitously expressed. CD40 is also expressed on many cell types. However, in terms of its role in adaptive immune responses, perhaps the most important locations are on the surface of DC and B cells. Interestingly, FcγRIIB is the only FcγR expressed on B cells, whereas both activatory and inhibitory FcγR are present on mouse DC. Thus, it is tempting to speculate that the in vivo activity of anti-CD40 is mediated through B cells, in which a locally high
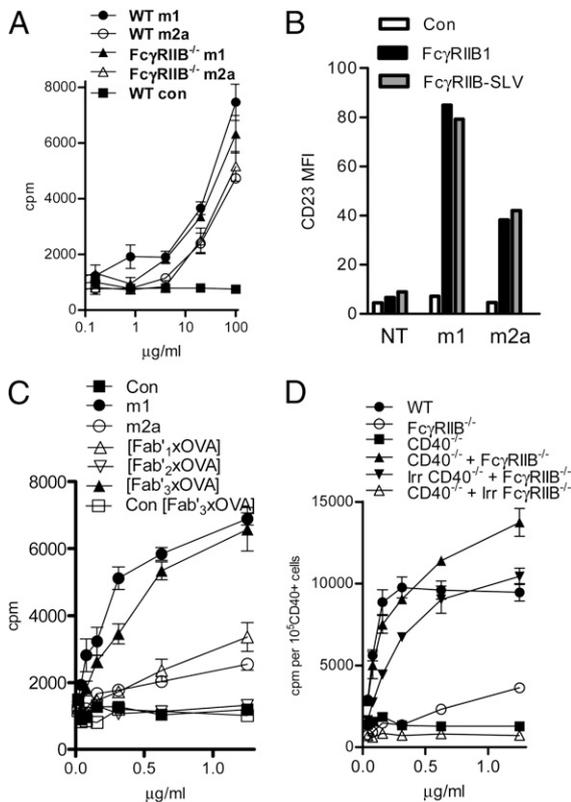
FIGURE 5. The role of FcγRIIB is in Ab cross-linking. *A*, Different concentrations of 3/23 m1 and m2a or m1 isotype control (con) were coated onto plastic overnight before incubation with WT or FcγRIIB$^{-/-}$ B cells. B cell proliferation was assessed as in Fig. 3*C*. Results are mean ± SEM of triplicate wells and show one out of two independent experiments. *B*, Control (Con) mouse B cell lymphoma cells or cells transfected with full-length mouse FcγRIIB1 or a truncated FcγRIIB lacking its intracellular tail (FcγRIIB-SLV) were incubated for 24 h with or without (NT) 10 μg/ml 3/23 m1 or m2a. Surface expression of CD23 was analyzed by flow cytometry. *C*, WT B cell proliferation in response to isotype control mAb (Con), 3/23 m1, or m2a [3/23 F(ab′)$_3$ × OVA], [3/23 F(ab′)$_2$ × OVA], [3/23 F(ab′)$_1$ × OVA], or [F(ab′)$_3$ × OVA] targeted to MHC II (con [F(ab′)$_3$ × OVA]) was assessed as described in Fig. 3*C*. Results are mean ± SEM for triplicate samples from one out of four independent experiments. *D*, WT, FcγRIIB$^{-/-}$ and CD40$^{-/-}$ B cells either untreated or irradiated (Irr) to prevent proliferation were incubated with increasing concentrations of 3/23 m1. A single cell type or two cell types were mixed as indicated. B cell proliferation was assessed as described for Fig. 3*C*. Results are counts per 10^5 CD40$^+$ cells/well, except when FcγRIIB$^{-/-}$ cells were used alone, for which results for 10^5 total cells are shown. Results are mean ± SEM for triplicate samples and are from one out of two independent experiments.

concentration of FcγRIIB would be present (e.g., in B cell follicles). Its direct action on B cells could explain its potent ability to stimulate humoral immunity and also T cell responses, as activated B cells have been demonstrated to act as APC for both CD4 and CD8 T cells (51, 52). Indeed, preliminary data suggest that prior depletion of B cells with anti-CD20 mAb prevents the stimulatory effect of 3/23 m1 on CD8 T cell expansion (not shown). Future experiments, involving mouse models in which FcγRIIB is selectively knocked out on B cells or DC, will be used to address the site of anti-CD40 action in vivo.

A possible explanation for the lack of immunostimulatory activity of 3/23 m2a was that this mAb depleted CD40-positive cells, much as anti-CD20 m2a depletes B cells in mice (6). We believe this was not the case, however, as: 1) the transient decrease in numbers of circulating B cells was similar in 3/23 m1- and m2a-
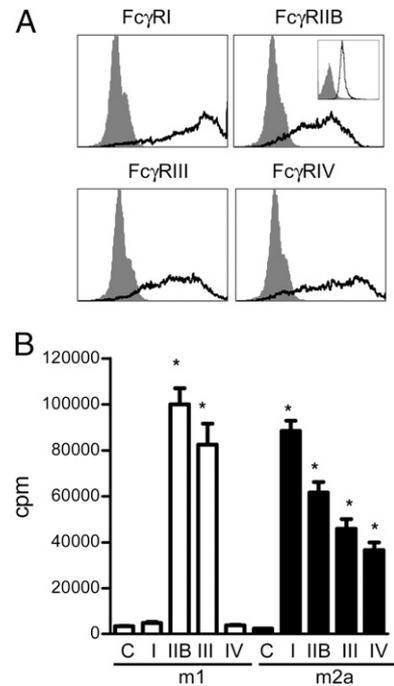
FIGURE 6. Other Fc receptors can also provide cross-linking for anti-CD40. *A*, 293F cells were transfected with the different mouse FcγRs as indicated and levels of expression analyzed by flow cytometry. Histograms represent untransfected (gray filled histogram) and FcγR-transfected cells (black line) stained with the relevant FITC-labeled mAb. *Inset* in the FcγRIIB histogram shows levels of FcγRIIB expression on WT splenic B cells. *B*, FcγRIIB$^{-/-}$ B cells were incubated with untransfected 293 cells (C) or cells transfected as in *A* plus 625 ng/ml 3/23 m1 or m2a and proliferation assessed as in Fig. 3*C*. Results are mean ± SEM for triplicate samples and represent one out of three independent experiments. *p ≤ 0.001 versus control.

treated animals (Fig. 1*E*); 2) there was no evidence that 3/23 m2a depleted adoptively transferred CFSE-labeled B cells from the spleen (Fig. 3*B*); 3) numbers of B cells and DC in the spleen were similar in 3/23 m2a-treated and control mice (Figs. 1*E*, 3*A* and data not shown); and 4) 3/23 m2a did not inhibit B or T cell responses (Fig. 2), as might be expected if this mAb depleted CD40-positive cells. In fact, our data suggested some limited stimulatory activity of 3/23 m2a, as it caused a detectable, albeit small and reproducible, increase in CD70 expression on splenic DC and also a small, but significant, increase in OVA-specific CD4 T cell expansion, consistent with the expression of activatory FcγR on DC.

A crucial question is how our results may be translated to the human system, in which there are clear differences from mice in terms of mAb isotypes and their interaction with FcγR (41, 50). The positive role of activatory receptors (FcγRIIa and -IIIa) in the activity of direct binding anti-cancer mAb in humans has been confirmed through analysis of drug responses in patients with polymorphisms in these receptors (10–13). As a result, much research has been focused on the engineering of mAb that have enhanced activatory FcγR binding and A/I ratios (14, 15). Our studies suggest that this may not be the best approach for anti-CD40 mAb and by extension possibly other immunostimulatory agents and cancer-binding mAb. Once these agents reach the clinic, similar genetic studies to those conducted for rituximab, alemtuzumab, and cetuximab (10–13) in humans would be required to address this. It would be of particular interest to examine responses in patients with different alleles of FcγRIIB shown to influence either levels of receptor expression or incorporation into

lipid rafts, which may influence cross-linking function (53). Interestingly, of the anti-human CD40 mAb currently in clinical trials, CP870,893 is the most agonistic. This mAb has a human IgG2 Fc region, whereas the others have IgG1. This is intriguing, as human IgG2 is reported to bind less well than IgG1 to all FcγR (50). Clearly, further studies are required to determine the contribution of epitope specificity, mAb isotype, and FcγR interaction in the activity of anti-human CD40 mAb.

In conclusion, our studies in mice confirm a crucial role for FcγR in the activity of immunostimulatory anti-CD40 mAb. However, in stark contrast to direct-targeting anti-cancer mAb that require interaction with activatory FcγR (6), we demonstrate an essential role for the inhibitory receptor, FcγRIIB, in anti-CD40 activity. Future studies will be required to determine whether our observations can be extended to humans or to other immunostimulatory agents, some of which are already in clinical trials (19). These findings have important implications when considering the design of optimally active mAb based therapeutics.

Acknowledgments

Disclosures

The authors have no financial conflicts of interest.

References

1. Hudis, C. A. 2007. Trastuzumab—mechanism of action and use in clinical practice. *N. Engl. J. Med.* 357: 39–51.
2. Lim, S. H., S. A. Beers, R. R. French, P. W. Johnson, M. J. Glennie, and M. S. Cragg. 2010. Anti-CD20 monoclonal antibodies: historical and future perspectives. *Haematologica* 95: 135–143.
3. Clynes, R. A., T. L. Towers, L. G. Presta, and J. V. Ravetch. 2000. Inhibitory Fc receptors modulate in vivo cytoxicity against tumor targets. *Nat. Med.* 6: 443–446.
4. Uchida, J., Y. Hamaguchi, J. A. Oliver, J. V. Ravetch, J. C. Poe, K. M. Haas, and T. F. Tedder. 2004. The innate mononuclear phagocyte network depletes B lymphocytes through Fc receptor-dependent mechanisms during anti-CD20 antibody immunotherapy. *J. Exp. Med.* 199: 1659–1669.
5. Minard-Colin, V., Y. Xiu, J. C. Poe, M. Horikawa, C. M. Magro, Y. Hamaguchi, K. M. Haas, and T. F. Tedder. 2008. Lymphoma depletion during CD20 immunotherapy in mice is mediated by macrophage FcgammaRI, FcgammaRIII, and FcgammaRIV. *Blood* 112: 1205–1213.
6. Beers, S. A., R. R. French, H. T. Chan, S. H. Lim, T. C. Jarrett, R. M. Vidal, S. S. Wijayaweera, S. V. Dixon, H. Kim, K. L. Cox, et al. 2010. Antigenic modulation limits the efficacy of anti-CD20 antibodies: implications for antibody selection. *Blood* 115: 5191–5201.
7. Hamaguchi, Y., Y. Xiu, K. Komura, F. Nimmerjahn, and T. F. Tedder. 2006. Antibody isotype-specific engagement of Fcgamma receptors regulates B lymphocyte depletion during CD20 immunotherapy. *J. Exp. Med.* 203: 743–753.
8. Xu, Y., A. J. Szalai, T. Zhou, K. R. Zinn, T. R. Chaudhuri, X. Li, W. J. Koopman, and R. P. Kimberly. 2003. Fc gamma Rs modulate cytotoxicity of anti-Fas antibodies: implications for agonistic antibody-based therapeutics. *J. Immunol.* 171: 562–568.
9. Nimmerjahn, F., and J. V. Ravetch. 2005. Divergent immunoglobulin g subclass activity through selective Fc receptor binding. *Science* 310: 1510–1512.
10. Cartron, G., L. Dacheux, G. Salles, P. Solal-Celigny, P. Bardos, P. Colombat, and H. Watier. 2002. Therapeutic activity of humanized anti-CD20 monoclonal antibody and polymorphism in IgG Fc receptor FcgammaRIIIa gene. *Blood* 99: 754–758.
11. Weng, W. K., and R. Levy. 2003. Two immunoglobulin G fragment C receptor polymorphisms independently predict response to rituximab in patients with follicular lymphoma. *J. Clin. Oncol.* 21: 3940–3947.
12. Bibeau, F., E. Lopez-Crapez, F. Di Fiore, S. Thezenas, M. Ychou, F. Blanchard, A. Lamy, F. Penault-Llorca, T. Frébourg, P. Michel, et al. 2009. Impact of FcgammaRIIa-FcgammaRIIIa polymorphisms and KRAS mutations on the clinical outcome of patients with metastatic colorectal cancer treated with cetuximab plus irinotecan. *J. Clin. Oncol.* 27: 1122–1129.
13. Musolino, A., N. Naldi, B. Bortesi, D. Pezzuolo, M. Capelletti, G. Missale, D. Laccabue, A. Zerbini, R. Camisa, G. Bisagni, et al. 2008. Immunoglobulin G fragment C receptor polymorphisms and clinical efficacy of trastuzumab-based therapy in patients with HER-2/neu-positive metastatic breast cancer. *J. Clin. Oncol.* 26: 1789–1796.
14. Desjarlais, J. R., G. A. Lazar, E. A. Zhukovsky, and S. Y. Chu. 2007. Optimizing engagement of the immune system by anti-tumor antibodies: an engineer's perspective. *Drug Discov. Today* 12: 898–910.
15. Nimmerjahn, F., and J. V. Ravetch. 2007. Antibodies, Fc receptors and cancer. *Curr. Opin. Immunol.* 19: 239–245.
16. Tutt, A. L., R. R. French, T. M. Illidge, J. Honeychurch, H. M. McBride, C. A. Penfold, D. T. Fearon, R. M. Parkhouse, G. G. Klaus, and M. J. Glennie. 1998. Monoclonal antibody therapy of B cell lymphoma: signaling activity on tumor cells appears more important than recruitment of effectors. *J. Immunol.* 161: 3176–3185.
17. Beers, S. A., C. H. Chan, R. R. French, M. S. Cragg, and M. J. Glennie. 2010. CD20 as a target for therapeutic type I and II monoclonal antibodies. *Semin. Hematol.* 47: 107–114.
18. Wilson, N. S., B. Yang, A. Yang, S. Loeser, S. Marsters, D. Lawrence, Y. Li, R. Pitti, K. Totpal, S. Yee, et al. 2011. An Fcγ receptor-dependent mechanism drives antibody-mediated target-receptor signaling in cancer cells. *Cancer Cell* 19: 101–113.
19. Hodi, F. S., S. J. O'Day, D. F. McDermott, R. W. Weber, J. A. Sosman, J. B. Haanen, R. Gonzalez, C. Robert, D. Schadendorf, J. C. Hassel, et al. 2010. Improved survival with ipilimumab in patients with metastatic melanoma. *N. Engl. J. Med.* 363: 711–723.
20. French, R. R., H. T. Chan, A. L. Tutt, and M. J. Glennie. 1999. CD40 antibody evokes a cytotoxic T-cell response that eradicates lymphoma and bypasses T-cell help. *Nat. Med.* 5: 548–553.
21. Shrikant, P., A. Khoruts, and M. F. Mescher. 1999. CTLA-4 blockade reverses CD8+ T cell tolerance to tumor by a CD4+ T cell- and IL-2-dependent mechanism. *Immunity* 11: 483–493.
22. Sotomayor, E. M., I. Borrello, E. Tubb, F. M. Rattis, H. Bien, Z. Lu, S. Fein, S. Schoenberger, and H. I. Levitsky. 1999. Conversion of tumor-specific CD4+ T-cell tolerance to T-cell priming through in vivo ligation of CD40. *Nat. Med.* 5: 780–787.
23. French, R. R., V. Y. Taraban, G. R. Crowther, T. F. Rowley, J. C. Gray, P. W. Johnson, A. L. Tutt, A. Al-Shamkhani, and M. J. Glennie. 2007. Eradication of lymphoma by CD8 T cells following anti-CD40 monoclonal antibody therapy is critically dependent on CD27 costimulation. *Blood* 109: 4810–4815.
24. Tutt, A. L., L. O'Brien, A. Hussain, G. R. Crowther, R. R. French, and M. J. Glennie. 2002. T cell immunity to lymphoma following treatment with anti-CD40 monoclonal antibody. *J. Immunol.* 168: 2720–2728.
25. Todryk, S. M., A. L. Tutt, M. H. Green, J. A. Smallwood, N. Halanek, A. G. Dalgleish, and M. J. Glennie. 2001. CD40 ligation for immunotherapy of solid tumours. *J. Immunol. Methods* 248: 139–147.
26. Vonderheide, R. H. 2007. Prospect of targeting the CD40 pathway for cancer therapy. *Clin. Cancer Res.* 13: 1083–1088.
27. Beatty, G. L., E. G. Chiorean, M. P. Fishman, B. Saboury, U. R. Teitelbaum, W. Sun, R. D. Huhn, W. Song, D. Li, L. L. Sharp, et al. 2011. CD40 agonists alter tumor stroma and show efficacy against pancreatic carcinoma in mice and humans. *Science* 331: 1612–1616.
28. van Kooten, C., and J. Bancharau. 2000. CD40-CD40 ligand. *J. Leukoc. Biol.* 67: 2–17.
29. Grewal, I. S., and R. A. Flavell. 1998. CD40 and CD154 in cell-mediated immunity. *Annu. Rev. Immunol.* 16: 111–135.
30. Eliopoulos, A. G., and L. S. Young. 2004. The role of the CD40 pathway in the pathogenesis and treatment of cancer. *Curr. Opin. Pharmacol.* 4: 360–367.
31. Vonderheide, R. H., K. T. Flaherty, M. Khalil, M. S. Stumacher, D. L. Bajor, N. A. Hutnick, P. Sullivan, J. J. Mahany, M. Gallagher, A. Kramer, et al. 2007. Clinical activity and immune modulation in cancer patients treated with CP-870,893, a novel CD40 agonist monoclonal antibody. *J. Clin. Oncol.* 25: 876–883.
32. Advani, R., A. Forero-Torres, R. R. Furman, J. D. Rosenblatt, A. Younes, H. Ren, K. Harrop, N. Whiting, and J. G. Drachman. 2009. Phase I study of the humanized anti-CD40 monoclonal antibody dacetuzumab in refractory or recurrent non-Hodgkin's lymphoma. *J. Clin. Oncol.* 27: 4371–4377.
33. Luqman, M., S. Klabunde, K. Lin, G. V. Georgakis, A. Cherukuri, J. Holash, C. Goldbeck, X. Xu, E. E. Kadel, III, S. H. Lee, et al. 2008. The antileukemia activity of a human anti-CD40 antagonist antibody, HCD122, on human chronic lymphocytic leukemia cells. *Blood* 112: 711–720.
34. Johnson, P. W., N. M. Steve, F. Chowdhury, J. Dobbyn, E. Hall, and M. Ashton-KeyHodges, E., C. H. Ottensmeier, A. Williams, and M. Glennie. 2010. A Cancer Research UK phase I study evaluating safety, tolerability, and biological effects of chimeric anti-CD40 monoclonal antibody (MAb), Chi Lob 7/4. *J. Clin. Oncol.* 28(suppl): 2507.
35. Donepudi, M., D. D. Quach, and M. B. Mokyr. 1999. Signaling through CD40 enhances cytotoxic T lymphocyte generation by CD8+ T cells from mice bearing large tumors. *Cancer Immunol. Immunother.* 48: 153–164.
36. Boulanger, D. S., R. Oliveira, L. Ayers, S. H. Prior, E. James, A. P. Williams, and T. Elliott. 2010. Absence of tapasin alters immunodominance against a lymphocytic choriomeningitis virus polytope. *J. Immunol.* 184: 73–83.
37. Castro, F. V., A. L. Tutt, A. L. White, J. L. Teeling, S. James, R. R. French, and M. J. Glennie. 2008. CD11c provides an effective immunotarget for the generation of both CD4 and CD8 T cell responses. *Eur. J. Immunol.* 38: 2263–2273.
38. White, A. L., A. L. Tutt, S. James, K. A. Wilkinson, F. V. Castro, S. V. Dixon, J. Hitchcock, M. Khan, A. Al-Shamkhani, A. F. Cunningham, and M. J. Glennie. 2010. Ligation of CD11c during vaccination promotes germinal centre induction and robust humoral responses without adjuvant. *Immunology* 131: 141–151.
39. Taraban, V. Y., S. Martin, K. E. Attfield, M. J. Glennie, T. Elliott, D. Elewaut, S. Van Calenbergh, B. Linclau, and A. Al-Shamkhani. 2008. Invariant NKT cells

promote CD8+ cytotoxic T cell responses by inducing CD70 expression on dendritic cells. *J. Immunol.* 180: 4615–4620.

40. Walshe, C. A., S. A. Beers, R. R. French, C. H. Chan, P. W. Johnson, G. K. Packham, M. J. Glennie, and M. S. Cragg. 2008. Induction of cytosolic calcium flux by CD20 is dependent upon B Cell antigen receptor signaling. *J. Biol. Chem.* 283: 16971–16984.

41. Nimmerjahn, F., P. Bruhns, K. Horiuchi, and J. V. Ravetch. 2005. FcgammaRIV: a novel FcR with distinct IgG subclass specificity. *Immunity* 23: 41–51.

42. Syam, S., P. Mero, T. Pham, C. A. McIntosh, P. Bruhns, and J. W. Booth. 2010. Differential recruitment of activating and inhibitory Fc gamma RII during phagocytosis. *J. Immunol.* 184: 2966–2973.

43. Mizuno, T., and T. L. Rothstein. 2005. B cell receptor (BCR) cross-talk: CD40 engagement creates an alternate pathway for BCR signaling that activates I kappa B kinase/I kappa B alpha/NF-kappa B without the need for PI3K and phospholipase C gamma. *J. Immunol.* 174: 6062–6070.

44. Pound, J. D., A. Challa, M. J. Holder, R. J. Armitage, S. K. Dower, W. C. Fanslow, H. Kikutani, S. Paulie, C. D. Gregory, and J. Gordon. 1999. Minimal cross-linking and epitope requirements for CD40-dependent suppression of apoptosis contrast with those for promotion of the cell cycle and homotypic adhesions in human B cells. *Int. Immunol.* 11: 11–20.

45. Hirano, M., R. S. Davis, W. D. Fine, S. Nakamura, K. Shimizu, H. Yagi, K. Kato, R. P. Stephan, and M. D. Cooper. 2007. IgEb immune complexes activate macrophages through FcgammaRIV binding. *Nat. Immunol.* 8: 762–771.

46. Takai, T., M. Ono, M. Hikida, H. Ohmori, and J. V. Ravetch. 1996. Augmented humoral and anaphylactic responses in Fc gamma RII-deficient mice. *Nature* 379: 346–349.

47. van Vugt, M. J., A. F. Heijnen, P. J. Capel, S. Y. Park, C. Ra, T. Saito, J. S. Verbeek, and J. G. van de Winkel. 1996. FcR gamma-chain is essential for both surface expression and function of human Fc gamma RI (CD64) in vivo. *Blood* 87: 3593–3599.

48. Smith, K. G., and M. R. Clatworthy. 2010. FcgammaRIIB in autoimmunity and infection: evolutionary and therapeutic implications. *Nat. Rev. Immunol.* 10: 328–343.

49. Haswell, L. E., M. J. Glennie, and A. Al-Shamkhani. 2001. Analysis of the oligomeric requirement for signaling by CD40 using soluble multimeric forms of its ligand, CD154. *Eur. J. Immunol.* 31: 3094–3100.

50. Bruhns, P., B. Iannascoli, P. England, D. A. Mancardi, N. Fernandez, S. Jorieux, and M. Daëron. 2009. Specificity and affinity of human Fcgamma receptors and their polymorphic variants for human IgG subclasses. *Blood* 113: 3716–3725.

51. Lund, F. E., and T. D. Randall. 2010. Effector and regulatory B cells: modulators of CD4(+) T cell immunity. *Nat. Rev. Immunol.* 10: 236–247.

52. Jiang, W., M. M. Lederman, C. V. Harding, and S. F. Sieg. 2011. Presentation of soluble antigens to CD8+ T cells by CpG oligodeoxynucleotide-primed human naive B cells. *J. Immunol.* 186: 2080–2086.

53. Espeli, M., H. A. Niederer, J. A. Traherne, J. Trowsdale, and K. G. Smith. 2010. Genetic variation, Fcγ receptors, KIRs and infection: the evolution of autoimmunity. *Curr. Opin. Immunol.* 22: 715–722.

54. Illidge, T., J. Honeychurch, A. Vandersteen, and M. Cragg. 2000. Radioimmunotherapy in the pi-BCL1 B cell lymphoma model: efficacy depends on more than targeted irradiation alone. *Cancer Biother. Radiopharm.* 15: 581–591.